PERIODICA POLYTECHNICA SER. MECH.ENG VOL. 36, NO. 2, PP. 135-152 (1992)

SIZE EFFECTS IN BRITTLE MATERIALS[1]

R. A. HELLER

Department of Engineering Science and Mechanics
Virginia Polytechnic Institute and State University

Received: October 20, 1992

1. Introduction

Brittle structural materials contain randomly spaced and oriented cracks with statistically distributed sizes throughout their bulk. When such materials are used in structural applications, the applied loads may induce stresses under whose influence the cracks will propagate.

It has been shown by several investigators [1–3] that the probability of finding larger cracks increases with the volume of the material and the chance that such cracks produce incipient failure also increases with large stresses. The statistical distribution that best describes the behaviour of such brittle structural components is the Weibull probability function [4].

The analysis leads, for simple structural components, to design equations analogous to those used for deterministic analysis with the advantage that the designer can pre-set the probability of failure at a desired low level. For more complicated structures a finite element stress analysis must be performed in a conventional manner, after which probability calculations may be performed with stored stress values and corresponding element sizes in addition to material properties as the required input.

The probabilistic analysis shows that various components may be designed with different safety factors, depending on their size and stress distribution, and still maintaining the same level of safety.

2.Chain Rule, Weakest Link Hypothesis

For a chain to survive, all links must survive 'Chain Rule'. If the reliability of the links is $L_1, L_2, \ldots, L_m$, the reliability of the Chain is,

[1] Based on the author's lecture given in the frame of the program 'Guest Professors at the Department of Technical Mechanics, Finno-Ugrian term, Spring 1992.'

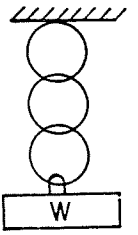

Fig. 1. The chain analogy

$$L = L_1 \times L_2 \times L_3 \times \cdots \times L_n.$$

2.1. Weibull Statistics

The probability that a *unit volume* (*Fig. 2*) of material survives under the application of a stress, S, is given as

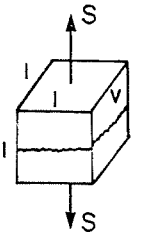

Fig. 2. Reliability of a unit volume

$$L(s) = e^{-\left(\frac{S}{R_c}\right)^m v}. \tag{1}$$

where $L(s)$ is the probability, R_c is the 'characteristic' ultimate strength of the unit or reference volume and, m is the Weibull shape parameter. These two constants define the two-parameter Weibull distribution (*Fig. 3*). The 'characteristic strength' has a probability of survival of $L(R_c) = e^{-1} = 0.37$. Some authors utilize the mean [1] or the median [3] strength in their derivations. Because the mean value is not associated with a specific probability level, it is not used here and for the sake of simplicity the 'characteristic value' will be utilized.

If the survival of the structural component requires that all volume elements survive and the elements are independent of each other, the reli-

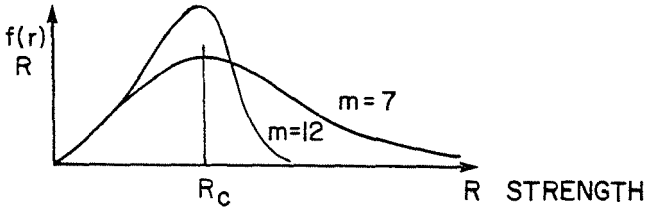

Fig. 3. Two-parameter Weibull distributions

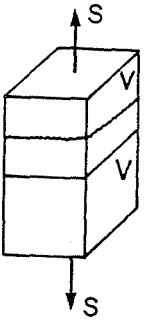

Fig. 4. Reliability of a series of unit volumes

ability of the component is equal to the product of the individual reliabilities of volume elements (weakest link hypothesis), as seen in *Fig. 4*.

$$L(Component) = e^{-\left(\frac{S_1}{R_c}\right)^m \cdot V_1} \cdot e^{-\left(\frac{S_1}{R_c}\right)^m \cdot V_2} \ldots e^{-\left(\frac{S_N}{R_c}\right)^m \cdot V_n} \tag{2}$$

or using the common base, e

$$L(Component) = e^{-\sum_{i=1}^{n}\left(\frac{S_i}{R_c}\right)^m \cdot V_i}. \tag{3}$$

For small volume elements the summation is replaced by integration (*Fig. 5*)

$$L(Component) = e^{-\int_v \left(\frac{S}{R_c}\right)^m \cdot dV} = e^{-\lambda}, \tag{4}$$

where the risk of failure, λ, the exponent of e, is called the stress-volume integral. If $S_{\max}$ is the maximum value of the applied stress through the

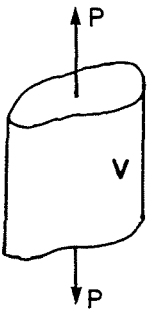

Fig. 5. Reliability of a continuum

component and V is its total volume, *Eq.* (4) may be written in terms of dimensionless ratios as

$$\ell \ln 1/L = \lambda = \left(\frac{S_{\max}}{R_c}\right) \cdot \frac{V}{v} \int_v \left(\frac{S}{S_{\max}}\right)^m \cdot \frac{dv}{V}. \tag{5}$$

In *Eq.* (5), R_c is the strength (characteristic value) of a *unit or reference volume*, v, of the material. The ratio

$$\frac{R_c}{S_{\max}} = \nu_c \tag{6}$$

is a safety factor referred to the characteristic strength of the reference volume and is called the *central safety factor.* The dimensionless variable $S/S_{\max}$ is independent of the volume for an elastic analysis; that is geometrically similar structures will have the same stress-volume integrals for any volume.

Substituting *Eq.* (6) into *Eq.* (5), two forms of the relation result

$$\ell n 1/L = \left(\frac{1}{\nu_c}\right)^m \left(\frac{V}{v}\right) \int_v \left(\frac{S}{S_{\max}}\right)^m \cdot \frac{dv}{V}, \tag{7}$$

$$\nu_c = \left\{ \frac{1}{\ell n 1/L} \cdot \frac{V}{v} \int_v \left(\frac{S}{S_{\max}}\right)^m \cdot \frac{dv}{V} \right\}^{1/m}. \tag{8}$$

Eq. (7) states that for a specified central safety factor, stress distribution and volume, the probability of survival or the probability of failure $P_f = 1 - L$ may be calculated.

According to *Eq.* (8), for a specified safety level, L, the required central safety factor, ν_c, is calculated.

3. Design Examples

3.1 Axial Tension or Compression

If a uniaxial force, P, is applied to a bar with a cross-sectional area A, (*Fig. 6*), the stress in the bar is uniform

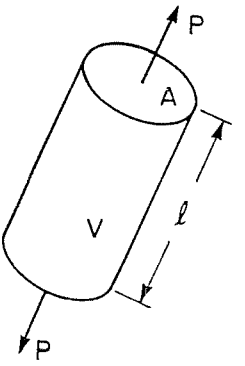

Fig. 6. Reliability of a bar subjected to tension

$$S = \frac{P}{A} = constant = S_{\max}$$

hence,

$$\frac{S}{S_{\max}} = 1, \int \left(\frac{S}{S_{\max}}\right)^m \cdot \frac{dv}{V} = 1$$

and substituting $\nu_c = R_c(P/A)$ into *Eq. 8*,

$$\ell n 1/L = \left(\frac{1}{\nu_c}\right)^m \cdot \frac{\ell \cdot A}{1}.$$

The probability of a failure is

$$P_f = 1 - L = 1 - e^{-\left(\frac{1}{\nu_c}\right)^m \cdot \frac{\pi \cdot D^2}{4} \cdot \ell} = 1 - e^{-\left(\frac{P/A}{R_c}\right)^m \cdot \frac{\pi \cdot D^2 \cdot \ell}{4}} = 1 - e^{-\frac{V}{\nu_c^m}}. \quad (9)$$

Eq. (9) can be used to illustrate size effect. It two different volumes V_1 and V_2 have the same reliabilities

$$L_1 = e^{-\frac{V_1}{\nu_1^m}} = L_2 = e^{-\frac{V_2}{\nu_2^m}}$$

then

$$\frac{V_1}{V_2} = \left(\frac{\nu_1}{\nu_2}\right)^m = \left(\frac{S_2}{S_1}\right),$$

therefore

$$S_1 = S_2 \left(\frac{V_2}{V_1} \right)^{1/m}. \tag{10}$$

If, for example, $V_2/V_1 = 100$ and $m = 12$, S_1, the strength of the smaller volume is 1.468 times greater than that of the larger one. Under uniaxial compression both the applied stress and the compressive strength of a reference volume are negative (usually numerically greater than the tensile strength) and the same relations apply.

3.2 Rectangular Cantilever Beam with Uniform Load

The bending moment in the beam (*Fig. 7*) is a function of x:

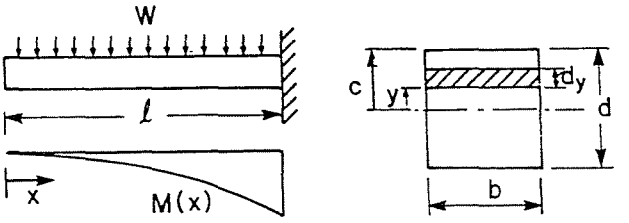

Fig. 7. Uniformly loaded cantilever beam

$$M(x) = -\frac{w \cdot x^2}{2}.$$

The corresponding stress is given in terms of the moment of inertia $I = bd^3/12$ as

$$S(x, y) = \pm \frac{w \cdot x^2}{2} \cdot \frac{d/2}{b \cdot d^3/12}.$$

The maximum stress occurs at the fixed end on the surface where $x = \ell$ and $y = d/2$

$$S_{\max} = \pm \frac{w \cdot \ell^2}{2} \cdot \frac{d/2}{b \cdot d^3/12}.$$

Hence

$$S/S_{\max} = \frac{2x^2 \cdot y}{\ell^2 \cdot d}.$$

As the lower half of the beam is in compression, *Eq.* (7) will consist of two parts

$$\ell n 1/L = \left(\frac{1}{\nu_c} \right)^m \frac{V}{v} \left[\int_{V_T} \left(\frac{S}{S_{\max}} \right)^m \cdot \frac{dv}{V} + \int_{V_c} \left(\frac{S}{H \cdot S_{\max}} \right)^m \cdot \frac{dv}{V} \right], \tag{11}$$

where the factor H is the negative ratio of the compressive strength and the tensile strength

$$H = -\frac{R_{cc}}{R_{ct}}. \tag{12}$$

For the beam

$$\ell n \frac{1}{L} = \left(\frac{1}{\nu_c}\right)^m \frac{\ell \cdot b \cdot d}{1} \left[\int_0^{d/2} \int_0^{\ell} \left(\frac{2x^2 \cdot y}{\ell^2 \cdot d}\right)^m \frac{b \cdot dx \cdot dy}{b \cdot d \cdot \ell} + \right.$$

$$\left. + \int_{-d/2}^{0} \int_0^{\ell} \left(\frac{2x^2 \cdot y}{H \cdot \ell^2 \cdot d}\right)^m \cdot \frac{b\, dx\, dy}{b \cdot d \cdot \ell} \right].$$

Performation of the indicated integrations results in

$$\ell n 1/L = \left(\frac{1}{\nu_c}\right)^m \frac{\ell \cdot b \cdot d}{2(2m+1)(m+1)} \left[1 + \left(\frac{1}{H}\right)^m\right]. \tag{13}$$

Comparing the maximum stress capability of a cantilever beam with that of a tension component of identical volume at the same level of reliability, neglecting the $\frac{1}{H^m}$ term, we obtain

$$\frac{V}{\nu_T^m} = \frac{1}{\nu_B^m} \frac{V}{2(2m+1)(m+1)}$$

or

$$S_{B_{\max}} = S_T [2(2m+1)(m+1)]^{1/m}.$$

Using again $m = 12$,

$$S_{B_{\max}} = 1.72 S_T.$$

The strength of the beam is greater than that of the tension component because in the beam only a small volume at the fixed end near the top and bottom is highly stressed while the tension specimen carries the same stress throughout its complete volume.

The example indicates the effects of stress concentrations and stress gradients.

3.3. Thick Walled Cylinder Under Internal Pressure

$$\left.\begin{aligned} S_T &= \frac{p \cdot T_i^2}{r_0^2 - r_i^2}\left[1 - \frac{r_0^2}{r^2}\right] \\ S_\theta &= \frac{p \cdot r_i^2}{r_0^2 r_i^2}\left[1 + \frac{r_0^2}{r^2}\right] \\ S_z &= \frac{2\mu \cdot p \cdot r_i^2}{r_0^2 - r_i^2} \end{aligned}\right\}. \tag{14}$$

In the case of a multi-axial stress state the theory of independent action [2] is utilized. The theorem states that a volume element fails when one of stress components acting normally to an incipient crack exceeds the strength of the material in that direction (*Fig. 8*). Hence, *Eq.* (2) is modified as

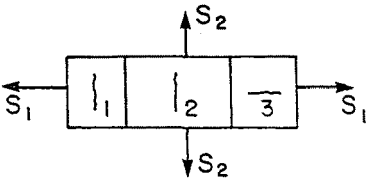

Fig. 8. Failure under a multi-dimensional state of stress

$$L(\Delta V) = e^{-\left(\frac{S_1}{R_1}\right)^m \cdot \Delta V} \cdot e^{-\left(\frac{S_2}{R_2}\right)^m \cdot \Delta V} \cdot e^{-\left(\frac{S_3}{R_3}\right)^m \cdot \Delta V},$$

$$L(Component) = L(\Delta V_1) \cdot L(\Delta V_2) \cdot \ldots L(\Delta V_n) \tag{15}$$

and hence

$$L(Component) = e^{-\sum_{i=1}^{3n}\left[\left(\frac{S_1}{R_1}\right)^m + \left(\frac{S_2}{R_2}\right)^m + \left(\frac{S_3}{R_3}\right)^m\right]\Delta V_i}. \tag{16}$$

The risk function, the exponent of *Eq. 15*, is again the stress-volume integral

$$\lambda = \int_v \left(\frac{S_1}{R_1}\right)^m \frac{dv}{v} + \int_v \left(\frac{S_2}{R_2}\right)^m \cdot \frac{dv}{v} + \int_v \left(\frac{S_3}{R_3}\right)^m \cdot \frac{dv}{v}, \tag{17}$$

where R_1, R_2 and R_3 are the strength components of the reference volume in the directions of the principal stresses S_1, S_2 and S_3. If the material is homogeneous and isotropic, $R_1 = R_2 = R_3 = R_c$.

$$\lambda = \left(\frac{|S_{\max}|}{R_c}\right)^m \cdot \frac{V}{v}\left[\int \left(\frac{S_1}{|S_{\max}|}\right)^m \cdot \frac{dv}{V} + \right.$$

$$\left. + \int \left(\frac{S_2}{|S_{\max}|}\right)^m \cdot \frac{dv}{V} + \int \left(\frac{S_3}{|S_{\max}|}\right)^m \cdot \frac{dv}{V}\right], \tag{18}$$

where $|S_{\max}|/R_c = 1/\nu_c$.

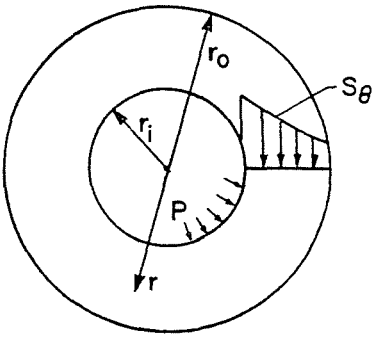

Fig. 9. Thick walled cylinder under internal pressure

For a cylinder with $r_0 = 6$ cm, $r_i = 4$ cm and $\ell = 100$ cm (*Fig. 9*) and $m = 7$, $\int_{V_r} = 3.79139 \cdot 10^{-11}$, $\int_{v_\theta} = 2.13794 \cdot 10^{-1}$, $\int_{V_z} = 4.27794 \cdot 10^{-7}$, $V = \pi \cdot \left(r_0^2 - r_i^2\right) \cdot \ell = 6283 \cdot$ cm^3, and $v = 1$ cm^3, hence

$$\lambda = \left(\frac{1}{\nu_c}\right)^7 \cdot 6283 \cdot [3.79139 \cdot 10^{-11} + 2.13794 \cdot 10^{-1} + 4.27794 \cdot 10^{-7}]$$
$$= 1.343 \cdot 10^3 \cdot \left(\frac{1}{\nu_c}\right)^7$$

It can be seen that only the tangential stress has a significant effect on the reliability of the cylinder. For a factor of safety $\nu_c = 5$ the reliability of the cylinder is $L = 0.983$.

3.4 Axially Loaded Notched Bar

The axially loaded notched bar (*Fig. 10*) is analyzed with the aid of a finite element program that calculates the maximum principal stresses at nine integration points (*Fig. 11*) in each element. The stresses and the corresponding surface areas are recorded. Once this has been accomplished, the largest maximum principal stress, $S_{\max}$, in the plate is searched out; each stress is divided by $S_{\max}$, the ratio is raised to the m^{th} power and is multiplied by the corresponding area and the plate thickness b. The term is then divided by the total volume and is summed up over all integration points to result in the finite element version of the stress volume integral

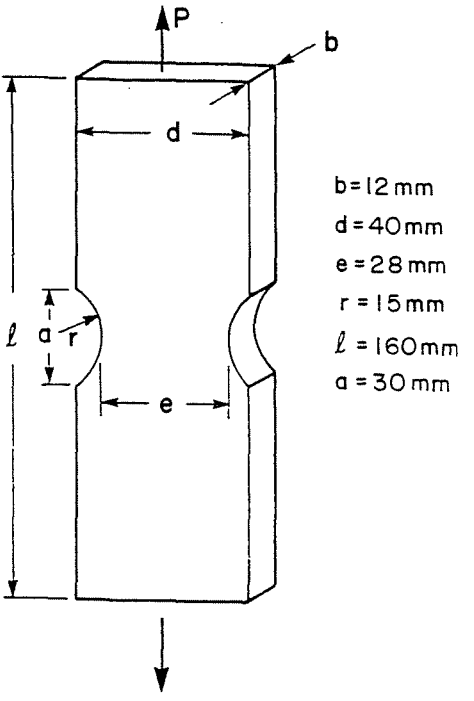

Fig. 10. Axially loaded notched bar

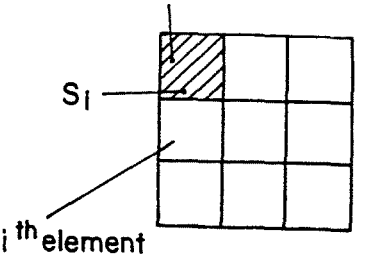

Fig. 11. Finite element notation

$$\int_v \left(\frac{S}{S_{\max}}\right)^m \cdot \frac{dv}{V} = \sum_{j=1}^{n} \sum_{i=1}^{q} \left(\frac{S_{ij}}{S_{\max}}\right)^m \cdot \frac{A_{ij} \cdot b}{V}. \tag{19}$$

The other principal stress will not contribute to the stress-volume integral and is hence neglected.

This summation is substituted into *Eq.* (7) for the risk function

$$\lambda = \ell n 1/L = \left(\frac{1}{\nu_c}\right) \cdot \frac{V}{v} \cdot \sum_{j=1}^{n} \sum_{i=1}^{g} \left(\frac{S_{ij}}{S_{\max}}\right)^m \cdot \frac{A_{ij} \cdot b}{V},$$

$$\ell n 1/L_{ij} = \left(\frac{1}{\nu_c}\right)^m \cdot \sum_{i=1}^{g} \left(\frac{S_{ij}}{S_{\max}}\right)^m \cdot A_{ij} b, \quad j = 1, 2, \ldots, n, \tag{20}$$

$$L = \prod_{j=1}^{n} L_j$$

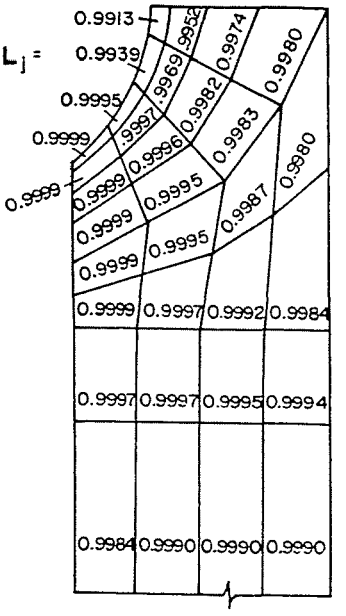

Fig. 12. Reliabilities of finite elements in a notched bar

A quarter of the plate, shown in *Fig. 12*, was analyzed and the reliabilities of the elements were calculated. The total reliability of the plate is then computed as

$$L_{1/4} = 0.95, \; L_{\text{plate}} = \left(L_{1/4}\right)^4 = 0.814.$$

4. Orthotropic Materials

4.1 Analysis of Orthotropic Materials

When the strength of the material varies with orientation, the orthotropic properties can be described by a strength ellipsoid where principal axes coincide with the material axes [2]. The directions of the three principal stress axes do not usually coincide with the material axes. Under such conditions it becomes necessary to perform a transformation of the strength in order to calculate three strength values in the directions of the three principal stresses (*Fig. 12*).

For an orientation defined by the direction cosines (l_1, l_2, l_3) of the principal stress S_1

$$R_{c1} = \left[\left(\frac{\ell_1}{R_c^{(1)}} \right)^2 + \left(\frac{\ell_2}{R_c^{(2)}} \right)^2 + \left(\frac{\ell_3}{R_c^{(3)}} \right)^2 \right]^{-1/2}, \tag{21}$$

where $R_c^{(1)}$, $R_c^{(2)}$, $R_c^{(3)}$ are the principal strengths along the material axes. Hence the 'Stress-Volume-Integral' of an anisotropic material is written as

$$\lambda = \frac{V}{v} \int \left[\left(\frac{S_1}{R_{c_1}} \right)^m \right] dv + \frac{v}{v} \int \left[\left(\frac{S_2}{R_{c_2}} \right)^m \right] \frac{dv}{v} + \frac{V}{v} \int \left[\left(\frac{S_3}{R_{c_3}} \right)^m \right] \frac{dv}{V} \tag{22}$$

In the case of a laminated composite material the three dimensional ellipsoid reverts to a strength ellipse.

Experiments conducted on a quasi-isotropic graphite epoxy laminate indicate such a directional variation of strength. The table shows such measurements [1].

The Weibull modulus is independent of direction within the material and for the particular material considered is approximately equal to $m = 26$ for all angles θ. The unit volume strengths depend on orientation and their magnitudes change by about 25 percent over the range $\theta = 0°$ to $\theta = 90°$. The best fit curve describing the variation of R_c with θ is an ellipse. An elliptic equation, with semi-major axes given by $R_c(0°) = 30.085$ and $R_c(90°) = 23.598$, (*Fig. 13*)

$$R_c(\theta) = \left[\frac{\cos^2 \theta}{R_c(0\,\mathrm{deg})^2} + \frac{\sin^2 \theta}{R_c(90\,\mathrm{deg})^2} \right]^{-1/2} \tag{23}$$

predicts strengths differing from the experimental values by 6 percent at the most (see *Fig. 14*). Generalizing these results confirms the transformation law postulated by *Eq.* (23).

Table 1
Weibull Moduli and Unit Volume Strengths for the Anisotropic Tests[1]

θ^0	Weibull Modulus m	$R_c(\theta)$Exp N/mm^2/cm^3	$R_c(\theta)Th$ N/mm^2/cm^3
0	25.0	30.08	30.08
10	25.7	30.80	29.80
20	22.1	29.45	29.04
30	24.9	29.32	27.97
40	27.3	28.30	26.81
50	26.3	26.60	26.73
60	22.2	24.72	24.82
70	23.0	23.78	24.14
80	28.1	23.98	23.55
90	26.5	23.59	23.59

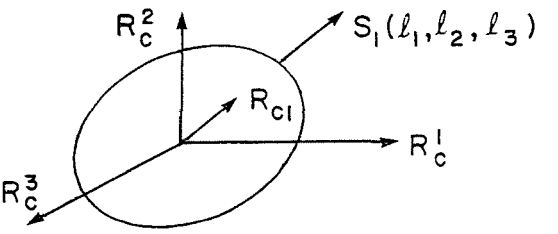

Fig. 13. Strength ellipsoid

4.2 Finite Element Formulation

Eq. 22 cannot usually be integrated in closed form and the point-by-point stress analysis may also be difficult to perform analytically. When a finite element stress analysis is used, the three principal stresses and their directions must be calculated and the volume of corresponding elements must be available. Three characteristic strength vectors in tension and compression are to be calculated in the directions of the principal stresses for each element (or for each integration point). The integrations of *Eq.* (22) are

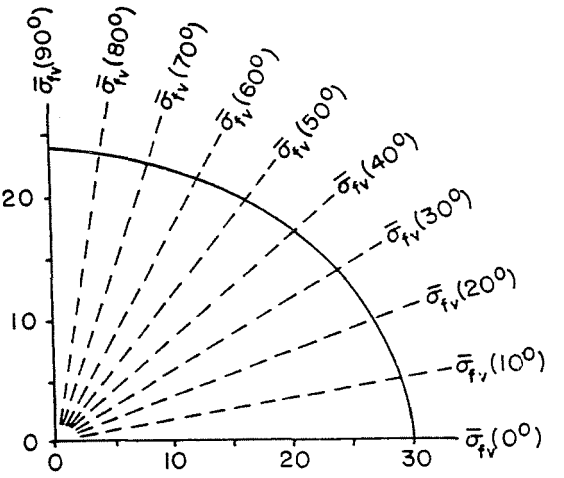

Fig. 14. Variation of reference volume strength with angle of anisotropy

then replaced by summations

$$\lambda_j = \sum l_{i=1}^{3} \left[\left(\frac{S_{ij}}{R_{cij}} \right)^{m'} \right] \frac{\Delta V_{ij}}{v} \tag{24}$$

The reliability of the structure consisting of n elements is the product of the reliabilities of elements and the risk of failure, λ, is the sum of the risks.

$$\lambda = \sum_{j=1}^{n} \lambda_j = \sum l_{j=1}^{n} \sum_{i=1}^{3} \left[\left(\frac{S_{ij}}{R_{cij}} \right)^{m'} \right] \frac{\Delta V_{ij}}{v} \tag{25}$$

and

$$L = \prod_{j=1}^{n} L_j = e^{-\lambda} \tag{25}$$

5. The Three-Parameter Weibull Distribution

It has been indicated in *Eq.* (10) that the strength of a smaller volume is greater than that of a larger one. That relationship also implies that the strength of a very large volume of material would be practically zero. Such a conclusion is unrealistic. This difficulty can be overcome with the introduction of a third parameter, R_0, the minimum strength, into the Weibull

distribution. In contrast to *Eq.* (1), the three-parameter distribution is written as

$$L = e^{-\left(\frac{S-R_0}{R_c-R_0}\right)^{m_v}}. \tag{26}$$

When *Eq.* (26) is used instead of *Eq.*(7), the relationship

$$\lambda = \ell n 1/L = \left(\frac{1}{\nu_c(1-1/\nu_{\max})}\right)^m \frac{V}{v} \int\limits_{S>R_0} \left(\frac{S}{S_{\max}} - \frac{\nu_c}{\nu_{\max}}\right)^m \frac{dv}{v} \tag{27}$$

results, where $\nu_{\max} = \frac{R_c}{R_0}$. *Eq.* (27) recognizes that most materials possess a minimum strength. When stresses below this level are applied no failure can occur. Integration in this case is carried out only for that portion of the volume for which the applied stress exceeds the minimum strength, R_0.

Accordingly, *Eq.* (10) is modified as

$$\frac{S}{R_c} = \left[\left(1 - \frac{R_0}{R_c}\right)\left(\frac{v}{V}\right)^{\frac{1}{m}} + \frac{R_0}{R_c}\right], \tag{28}$$

where R_c is the characteristic strength of the reference volume, v, and R_0 is the minimum strength.

If for a typical material $\frac{R_0}{R_c} = 0.6$ and $m = 12$, a volume 100 times larger than the reference volume will have a strength of $0.87\,R_c$. *Eq.* (10) would predict $0.68\,R_c$.

Even for a very large volume the strength would only drop to the R_0 value.

The three-parameter version, *Eq.* (27) can be used to replace any of the relevant relations in the foregoing examples.

6. Experimental Verification of Size Effects

It is evident from *Eq.* (28) that in order to demonstrate size effects experimentally, large volume ratios are required. Small laboratory specimens can be tested in statistically significant quantities but full size structural components are too expensive and cannot be replicated in sufficient numbers.

To circumvent this problem, size effects can be demonstrated by relying on specimens containing severe stress gradients as demonstrated in Section 3.2.

Consequently, notched specimens have been prepared as shown in *Fig. 15.* In these specimens stresses are high in a small volume at the tip of the notch. Results of four-point bending tests on such notched specimens

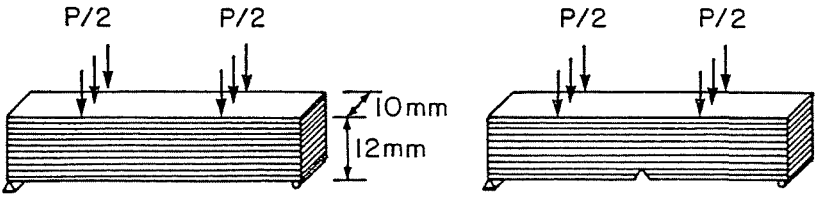

Fig. 15. Smooth and notched beams loaded in four-point bending

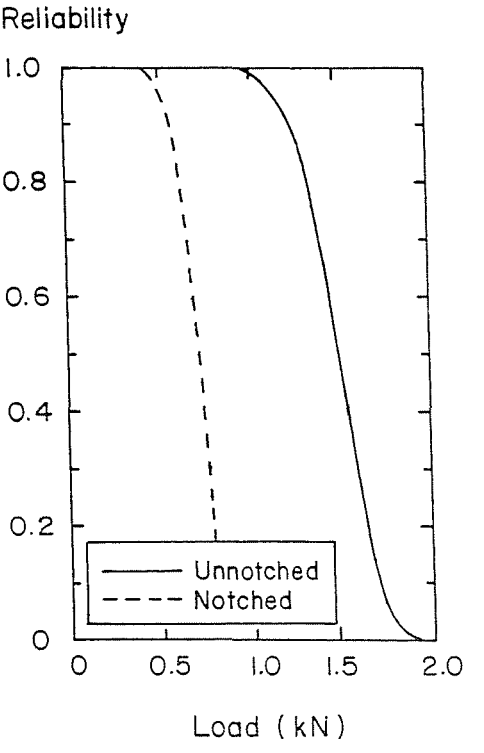

Fig. 16. Comparison of smooth and notched beam reliabilities as functions of load

are compared with smooth beams (large volume) of the same size. In this manner, volume ratios of the order of 1000 may be achieved.

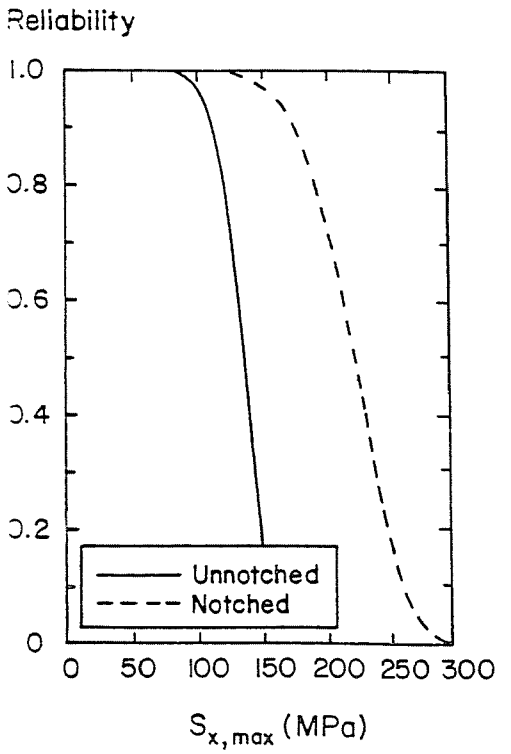

Fig. 17. Comparison of smooth and notched beam reliabilities as functions of failure stress

Both types of beams are subjected to a finite element stress analysis, failure loads are measured in a testing machine as well as experimental and analytical loads are compared. If the calculated loads agree with the experimentally obtained ones, the analytical stresses are assumed to be correct.

Small beams of a composite material as shown in *Fig. 15* have been machined and tested. Calculated failure loads and maximum stresses versus reliability are presented in *Figs. 16* and *17*. It can be seen that at a 50% reliability value the load carrying capacity of the notched beams is about half of that of smooth beams, a result that agrees with experiments. On the other hand, the maximum stress at failure in notched beams is 1.8 times greater than the strength of unnotched beams, a clear indication of size effect.

7. Conclusions

The strength reduction in large components as compared to laboratory size specimens has been demonstrated based on the 'Weakest Link' hypothesis and the Weibull distribution. Calculations of such size effects for various simple structural components have been carried out in closed form and with the aid of Finite Element Analysis for more complicated structures.

Experiments performed on notched and unnotched composite beams have been used to verify the results.

References

1. MAGETSON, J.: Failure Probability Evaluation of an Anisotropic Brittle Structure Derived from a Thermal Stress Solution in 'Thermal Stresses in Severe Environments', Ed. Hasselman and Heller, Plenum, New York, pp. 503–519 (1980).
2. STANLEY, P. – SIVILL, A. D. – FESSLER, H.: The Application and Confirmation of a Predictive Technique for the Fracture of Brittle Components, Paper No. 22, Proc. Fifth Int. Conf. on Exper. Stress Anal., Udine, Italy (1974).
3. CORDS, H. – DJALOEIS, A.Gl,– MONCH, J. – ÓFINGER, B. – ZIMMERMANN, R.: Bruchkriterien für Graphit, JUL–1355 Kernforschungsanlage Julich GmbH, October (1976).
4. WEIBULL, W. J.: *Applied Mechanics,* Vol. 18, (3), p. 293 (1951).

Address:

Robert A. HELLER, Ph.D.
Professor of Engineering Mechanics
Department of Engineering Science and Mechanics
Virginia Polytechnic Institute and State University
Blacksburg, VA 24061–0219, USA